

Sebastian Herrmann

Relevant Anatomy and Physiology of the Shoulder

While the term shoulder joint commonly refers to the glenohumeral joint, shoulder motion and stability are dependent on at least three joints and a multitude of bony and soft-tissue structures. The sternoclavicular (SC) joint is formed between the sternal end of the clavicle and the manubrium sterni. It represents the only “true” articulation between the torso and the lateral shoulder girdle. A strong joint capsule provides stability while allowing for clavicle motion around an anterior/posterior (elevation/depression), a vertical (protraction/retraction) and a longitudinal axis (rotation). The clavicle has a double-convex contour with a flattened shape lateral and a more tubular shape at its medial third. Laterally, it articulates with the acromial process of the scapula via the acromioclavicular (AC) joint. The clavicle not only acts as a strut, but also protects underlying neurovascular structures such as the subclavian blood vessels and the brachial plexus. Stability of the lateral clavicle is provided by both the coracoclavicular ligaments and the AC-joint capsule. Injury to these structures can lead to acromioclavicular instability, which often results in impaired scapular kinesis [1].

The scapula is positioned on the upper dorsolateral aspect of the thoraces. It is a flat, triangular-shaped bone. On its superolateral aspect, the coracoid process originates and then tracks anterolaterally. It acts as an origin to the coracoclavicular ligaments superiorly and the conjoint tendons anteriorly. Dorsally, the acromion arises from the spina scapulae, which then curves laterally and anteriorly. The coracoacromial ligament spans between the anterior facet of the

acromion and the lateral aspect of the coracoid process. This ligament is an important restraint to superior migration of the humeral head in normal shoulders and shoulders with rotator cuff disease [2, 3].

The glenoid fossa forms the socket part of the glenohumeral joint. Its shape and orientation are variable and should be evaluated before all arthroplasty procedures. The majority of healthy adults have a pear-shaped glenoid, whereas in nearly 30 % of healthy patients, the glenoid shape is elliptical [4]. Overall dimensions vary slightly with a mean width of about 24 mm for women and 28 mm for men, respectively. Its mean height is 33 mm for women and 38 mm for men [5]. Superiorly, the supraglenoidal tubercle forms the origin of the long head of the biceps, whereas inferiorly on the infraglenoidal tubercle the triceps brachii originates. The horizontal part between the glenoid fossa and the lateral scapular margin is referred to as scapular neck. Length of scapular neck is variable and can range from 5 to 19 mm with a mean of 10.5 mm. Recent studies suggest that a short scapular neck might contribute to the development of scapular notching following reversed shoulder arthroplasty (RSA) [6, 7].

Orientation of the glenoidal joint surface is commonly described as (retro-) version and inclination, whereas version describes orientation of the glenoidal cavity in relation to the scapular body in a coronal plane and inclination in relation to a transverse plane. Average inclination is -2.2° to 5.7° (positive values indicating a superior-facing glenoid) [5, 8]. Normal mid-glenoid version for healthy subjects averages $+2^\circ$ to -5.7° (negative values indicate retroversion), dependant on method of measurement [9–11]. The concave joint surface has a spiraling twist, with the superior parts being more retroverted than the inferior parts [9, 12]. This twist can sum up to a overall difference in retroversion of up to 11° between the upper and lower glenoid, which has to be taken into consideration, especially when assessing glenoid version in 2D-computed tomography images. In this case, the measured angles can vary significantly between each CT-slice. Position of the scapula relative to the CT scanner

S. Herrmann (✉)

Department of Orthopaedic and Trauma Surgery, Helios Klinikum
Emil von Behring, Walterhöferstr. 11, Berlin, 14165, Germany
e-mail: Sebastian.herrmann@helios-kliniken.de

S. Herrmann
Charité University of Medicine, Berlin, Germany

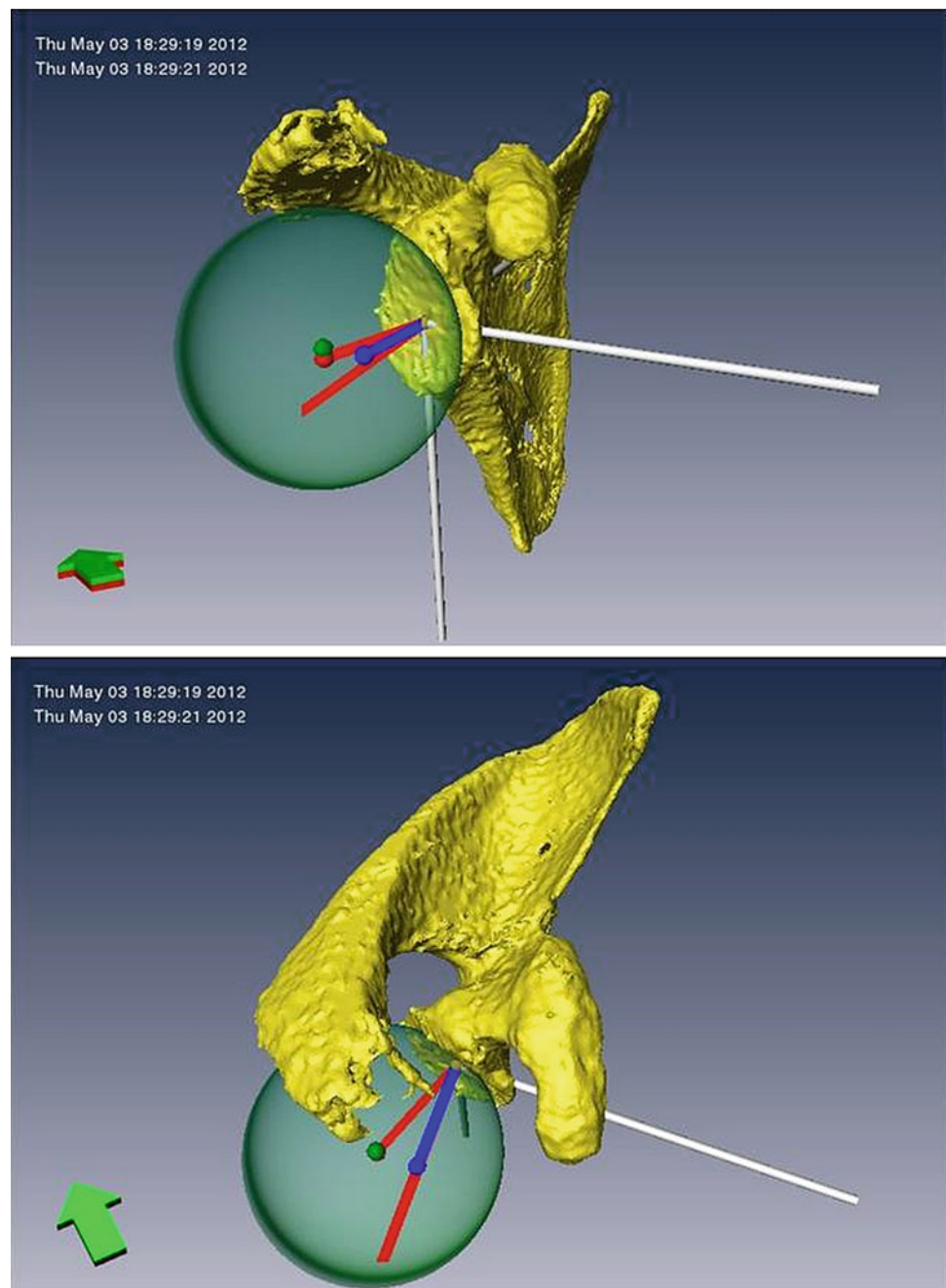
does also influence accuracy and relevant deviation from the actual in vivo situation might occur. Three-dimensional analysis of glenoid orientation has higher technical requirements but inaccuracy due to choice of CT-slice or shoulder-position relative to CT scanner can be avoided [13] (Fig. 2.1).

In arthritic shoulders, specific changes to glenoid orientation and morphology can be seen. While in patients with primary osteoarthritis, overall retroversion appears to be slightly bigger compared to normal shoulders, significantly less retroversion is seen in patients with cuff tear

arthropathy. Patients with cuff tear arthropathy and grade III or IV fatty infiltration of the infraspinatus or teres minor have an average of 3.6° glenoid retroversion, compared to 14.1° in patients with primary osteoarthritis and no significant fatty infiltration of rotator cuff muscles. On the other hand, patients with cuff tear arthropathy and grade III or IV fatty infiltration of the infraspinatus or teres minor have significantly less inclination as compared to patients with no significant fatty infiltration [14].

Walsh classified the specific changes of glenoid morphology in osteoarthritic shoulders. He differentiated three

Fig. 2.1 Evaluation of glenoid orientation using a sphere fit protocol in a three-dimensional CT-model of the scapula



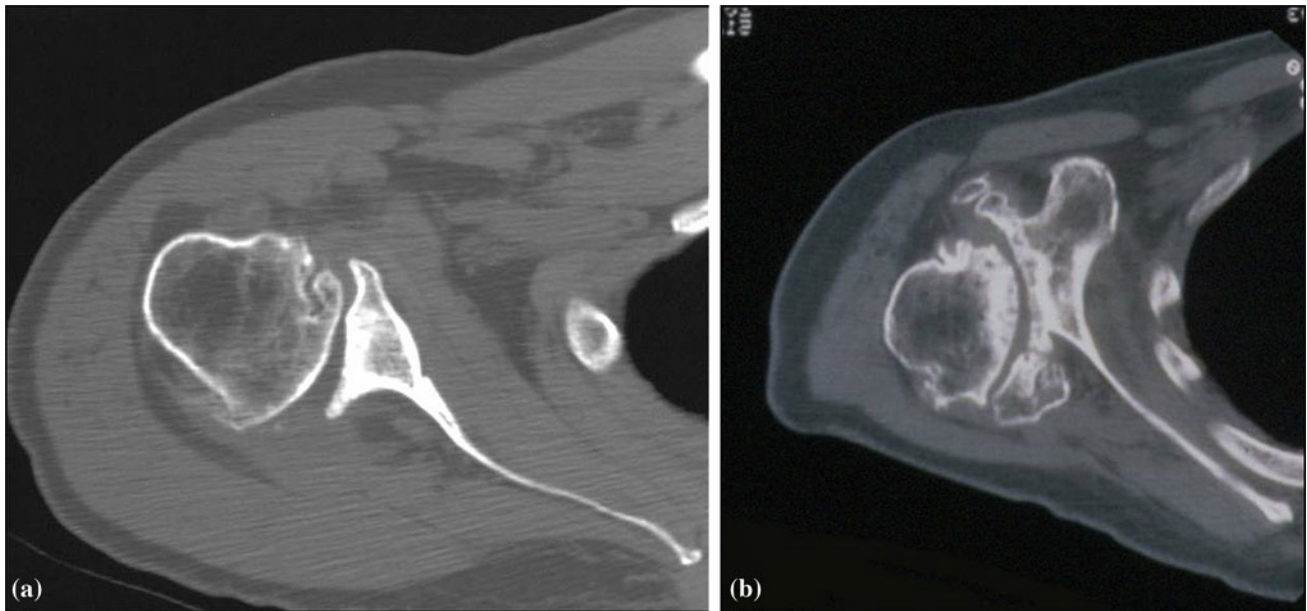


Fig. 2.2 Coronal CT-scan of arthritic shoulder with eccentric wear and biconcave-shaped glenoid (group B2 according to Walch) (a) and dysplastic glenoid with retroversion bigger 25° (Group C according to Walch) (b)

types: Group A represents a glenoid with central erosion, Group B shows posterior, excentric erosion due to subluxation of the humeral head, and Group C is a dysplastic glenoid with retroversion bigger 25° . Group B is further subdivided in group B1 where posterior sclerosis, joint space narrowing and osteophytes are present and group B2, where a biconcave aspect of the glenoid fossa is seen (Fig. 2.2) [15].

Anatomy of the proximal humerus is not less important, with a huge variety in all anatomic parameters seen in patients. The humeral head, which forms the ball of the glenohumeral joint, is more or less a true sphere. It has a mean diameter of 46–52 mm with a big range seen from 37 to 57 mm in healthy shoulders. There is a direct positive correlation between articular surface diameter and its height, which Boileau et al. defined as “the perpendicular distance from the articular margin to the apex of the diameter of curvature” [16]. Mean inclination angle as measured to the shaft axis is 130° , and its mean retroversion as measured to the transepicondylar axis is 18° . As the transepicondylar axis is difficult to determine in an intraoperative setting, the forearm axis can be taken as reference; however, in this case, a significant higher retroversion of 29° is noted [17]. Again both values show a high variance, with inclination angles varying between 120° and 135° and retroversion between -7° and 48° , respectively. Besides these angles, the humeral articular surface presents a posterior and medial offset relative to the shaft axis. The mean medial offset is 7 mm (3–11 mm), and the mean posterior offset is 2.6 mm (–1 to 6 mm).

Comparing the glenoidal and humeral articular surfaces, a mismatch in size is obvious: while overall glenoid surface

area averages about $5\text{--}9\text{ cm}^2$, the humeral head surface area is about three times bigger [18, 19]. However, contact area is increased by the labrum, which forms a fibrous ring surrounding the glenoid. The bony shape of the glenoid has a slightly smaller curvature compared to the humeral head. This mismatch is partly compensated by the cartilage, and therefore, humeral head and glenoid surface curvature are more or less congruent, with the difference being $<2\text{ mm}$ in the majority of patients [18].

The glenoid labrum and glenohumeral ligaments provide glenohumeral stability, while allowing an almost full circle range of motion. Therefore, their integrity, their position, and orientation are crucial. The glenoid labrum is a circumferential, fibrocartilaginous ring, attached to the glenoid rim. Superiorly, the long head of the biceps and the superior labrum form a complex known as the superior labrum anterior–posterior (SLAP). Lesions of the SLAP-complex can be a cause of shoulder pain especially in overhead athletes. These lesions were classified according to Snyder, who differentiates four subtypes. Maffet later described three more subtypes and extended the classification accordingly [20, 21]. Anteriorly, the superior and medial glenohumeral ligaments reach from the glenoid to the lesser tubercle and the inferior humeral neck. Beneath the medial glenohumeral ligament, the inferior glenohumeral ligament complex reaches downwards and laterally to its insertion on the proximal humerus. In contrast to the single-band structure of the superior and middle glenohumeral ligaments, the inferior ligament complex consists of two bands anteriorly and posteriorly and the axillary pouch in between [22].

The rotator cuff consists of four muscles. The supraspinatus (SSP) muscle originates from the supraspinatus fossa, tracks laterally underneath the acromion and finally inserts at the anterior–superior aspect of the greater tuberosity and in 20 % of patients also at the superior aspect of the lesser tuberosity [23]. Origin of the infraspinatus (ISP) muscle is the fossa infraspinatus on the dorsal aspect of the scapula. The muscle tracks superolateral and finds its insertion at the anterolateral aspect of the greater tuberosity. The footprint of the infraspinatus insertion is of trapezoidal shape and has a maximum length of about 10 mm mediolateral and 30 mm anteroposterior, respectively. Insertion of the teres minor is found at the most posterior and inferior facet of the greater tuberosity. Its origin is on the lateral margin of the scapula, just inferior and lateral to the infraspinatus muscle. Anteriorly, the subscapularis (SSC) muscles origin takes up almost the whole anterior scapula aspect. Its insertion at the lesser tuberosity is of trapezoidal shape, with a broad part superiorly and a thin, narrow part inferiorly. Overall dimensions of the tendinous insertion is about 18 mm width and 25 mm height [24], while muscular insertion is seen inferior to the lesser tuberosity, thus expanding the subscapularis insertion site distally [25].

The deltoid muscle is often referred to as the main engine of the shoulder. It has a triangular shape, with the base of the triangle being its origin on the lateral, anterior clavicle, the acromion, and the scapula spine [26]. Accordingly, the muscle consists of at least three parts: the anterior (clavicular), the lateral (middle) and the posterior (spinal) segments. However, some authors suggest an even greater segmentation, with four middle segments [27]. These segments find a wide insertion on the proximal, lateral humeral shaft. Distally, fascial connections with lateral intermuscular septum and the brachial fascia can be found, which will preserve deltoid function even in case of partial (anterior) release of the deltoid insertion [28]. Anteriorly, the deltoid fibers are adjacent to the pectoralis major muscle. This interval can easily be identified by the cephalic vein, which often will be surrounded by some fat tissue. Feeding vessels will radiate in the vein, with the majority of these vessels being laterally [29].

Biomechanics of Normal and Abnormal Shoulder Structures

The glenohumeral joint can be classified as an enarthrodial ball and socket joint. It allows polyaxial motion of the arm relative to the scapula. These motions can be described relative to the scapular plane in the following manner: humeral rotation around the sagittal axis is specified as abduction/adduction, rotation around the frontal axis, where the axis is directed in a medial–lateral direction, named

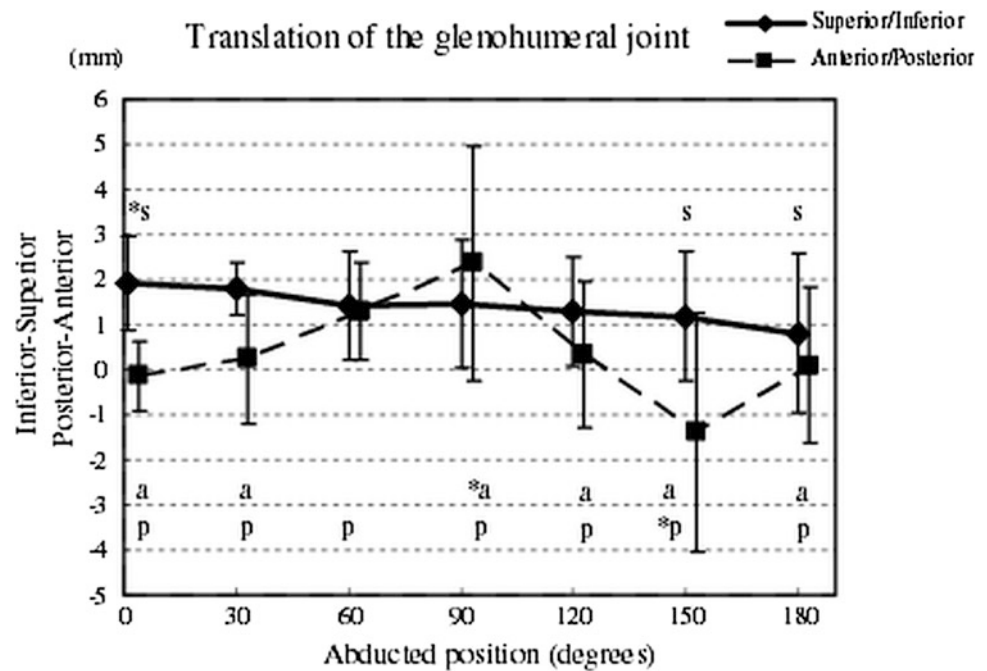
flexion/extension, and rotational movement around a longitudinal-humeral axis is referred to as external/internal rotation.

Even though articular surfaces are more or less congruent, glenohumeral joint kinematics do not fully equate enarthrodial kinematics. Exact determination of this kinematics has been subject to numerous studies. However, some controversy exists, and results are difficult to compare due to the variety of methodological approaches. Recently, development of open MRI and three-dimensional biplanar fluoroscopy techniques promise a highly increased accuracy and more realistic representation of the actual in vivo situation. Sahara et al. found an overall 1.1 mm inferior humeral translation during abduction using a vertically open MRI-technique. In the anterior–posterior direction, there was a 2.4 mm anterior translation while abduction from 0° to 90° and a posterior translation of −1.4 mm in abduction angles of 90°–150° (Fig. 2.3) [30]. Gibhart et al. found slightly bigger values with maximum superior–inferior translation of 4.2 ± 2.3 mm and 5.1 ± 1.1 mm for anterior–posterior translation, respectively.

These kinematics are highly dependable on the interaction of the rotator cuff, the deltoid and the scapulothoracic muscles. The anterior (SSC) and posterior (ISP/Teres minor) cuff act as a transverse force couple generating compressive forces. These glenohumeral joint reaction forces reach 45–90 % of total body weight, with the maximum forces seen in full abduction position. As a result, the humeral head is maintained centrally in the glenoid fossa, unaffected by the superior translational forces of the deltoid muscle [31]. The superior cuff (SSP) does also contribute to concavity compression, especially at early abduction [32]. However, with isolated supraspinatus tears, maximum joint compression forces remain unchanged, while tears of the anterior or posterior rotator cuff result in significantly decreased compression forces [33]. This decrease in compression forces leads to the inability to withstand the superior translational forces of the deltoid and superior migration of the humeral head might occur.

Motion of the arm is initiated by both the rotator cuff and the deltoid muscle. The muscle's capacity to generate a rotational force can be estimated by measurement of their moment arm respective to the particular axis. The deltoid muscle with its broad origin and big muscle mass is an effective abductor, external and internal rotator. When the arm is at the neutral, resting position, the lateral (middle) part of the deltoid has an abduction moment arm of about 16 mm, which is considerably smaller compared to the SSP abduction moment arm in this position (23 mm). However, with increasing abduction, this moment arm increases to 30–35 mm, making him the strongest abductor in this position. The bigger SSP moment arm at the resting position underlines its importance in initiating the abduction motion [34].

Fig. 2.3 Translation of the glenohumeral joint under load as measured in open MRI [30]



Humeral rotation is initiated by the anterior and posterior rotator cuff and deltoid portions. The subscapularis has an internal rotational moment arm of about 23 mm in the resting position making him the strongest internal rotator. Posteriorly, the Teres minor has a 17-mm external rotational moment arm and the infraspinatus 24-mm external rotation moment arm, respectively [35, 36]. The anterior and posterior subregions of the deltoid muscle contribute to rotational motion to a lesser degree in healthy shoulders, as their rotational moment arms are smaller with 4-mm external rotation moment arm for the posterior regions and 5-mm internal rotation moment arm for the anterior regions, respectively [37].

While the measurement of moment arms can give a rough estimation about the muscles capacity to generate rotational forces, other factors such as muscle tension and integrity should not be underestimated.

Joint and Muscle Forces in RSA

In RSA, the center of rotation (COR) is shifted medially and inferiorly. This shift affects biomechanical properties of the deltoid muscle and the remaining rotator cuff in various ways: First of all, the deltoid muscle gains tension. This tension is mandatory for prosthetic stability after RSA and does also increase sufficiency of the deltoid when initiating abduction. The total lengthening of the deltoid sums up to about 20 % compared to the normal shoulder [38]. In shoulders with cuff tear arthropathy, where there is a substantial cranialization of the humerus, this effect might even

be more pronounced. The medialization of the COR does also affect the deltoids abduction moment arm: While in healthy shoulders, an overall moment arm in respect to the sagittal axis of 16–35 mm can be seen [37, 39], it increases to 50–60 mm following RSA [38, 39]. Additionally, the amount of deltoid muscle fibres positioned lateral to the COR, which therefore have the capacity to create abducent forces increases with medialization of the COR [40]. On the other hand, a decrease of fibres positioned antero- or posteromedial to the COR, which have the potential to create internal or external, rotational forces in healthy shoulders, can be seen.

Analogous to the COR, the humerus with the insertion sites of the rotator cuff is shifted medially and inferiorly in conventional RSA. These changes have a significant influence on the biomechanical properties of the remaining rotator cuff. In patients with cuff tear arthropathy, supra- and infraspinatus seem to be the most commonly involved, whereas teres minor and subscapularis will often remain intact [41, 42]. Even though these muscles are strong external and internal rotators in healthy shoulders and their integrity might be maintained after RSA, humeral rotation often remains compromised or even decreases postoperatively [41, 43, 44]. While the decrease of deltoid fibres with rotational potential after RSA might be one contributing factor to these findings, a change to the biomechanical properties of the remaining rotator cuff has been identified as the other. Following conventional RSA, rotational moment arms of Teres minor show a significant decrease of up to 25 %, whereas the SSC rotational moment arms decrease by up to 36 % [36]. Moreover, muscle tension of both muscles,

especially at the resting position of the arm, declines. The overall decrease of muscle length after conventional RSA can be as high as 20 mm for the teres minor and 16 mm for the subscapularis. With increasing humeral abduction, the reduced muscle tension resolves, and the distal muscle segments might even have a minimal increased tension at abduction of 60° or more [36].

One potential way to address these disadvantageous biomechanical properties is to shift the COR laterally. Lateralization can be achieved by implant design or by interposition of an autologous bone block between the glenoid and the baseplate [2, 45]. While with these efforts a lateralization of 7–10 mm in comparison with the conventional

RSA is achieved, the COR is still shifted medially compared to normal shoulders. In lateralized RSA, rotational moment arms are preserved and no significant decrease of muscle tension for either SSC or teres minor is observed (Figs. 2.4 and 2.5). Only the very distal regions of the SSC show a slight decrease of muscle tension when the arm is in a 0° abduction position (139 mm vs. 145 mm) [46].

As mentioned before, joint reaction forces in healthy shoulders can be as high as 40–90 % of body weight, dependant on arm position and integrity of the rotator cuff. Following shoulder hemiarthroplasty, values of up to 238 % body weight were measured using an instrumented humeral implant [47]. After RSA, overall joint reaction forces are

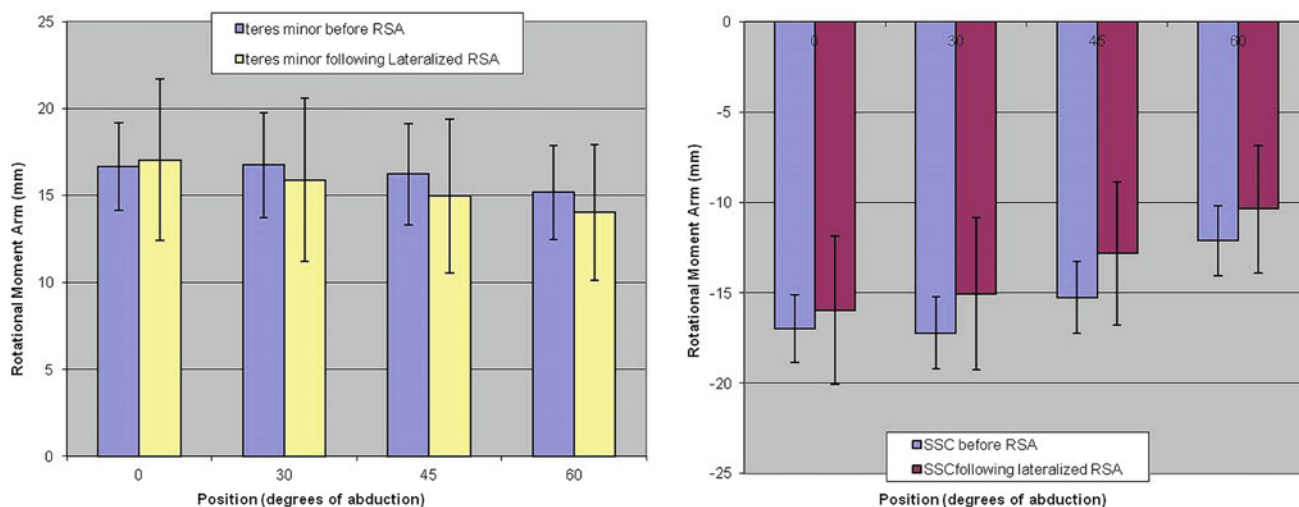


Fig. 2.4 Rotational moment arms (mm) of teres minor and subscapularis before and after lateralized RSA. No significant difference is seen for middle region of teres minor and subscapularis

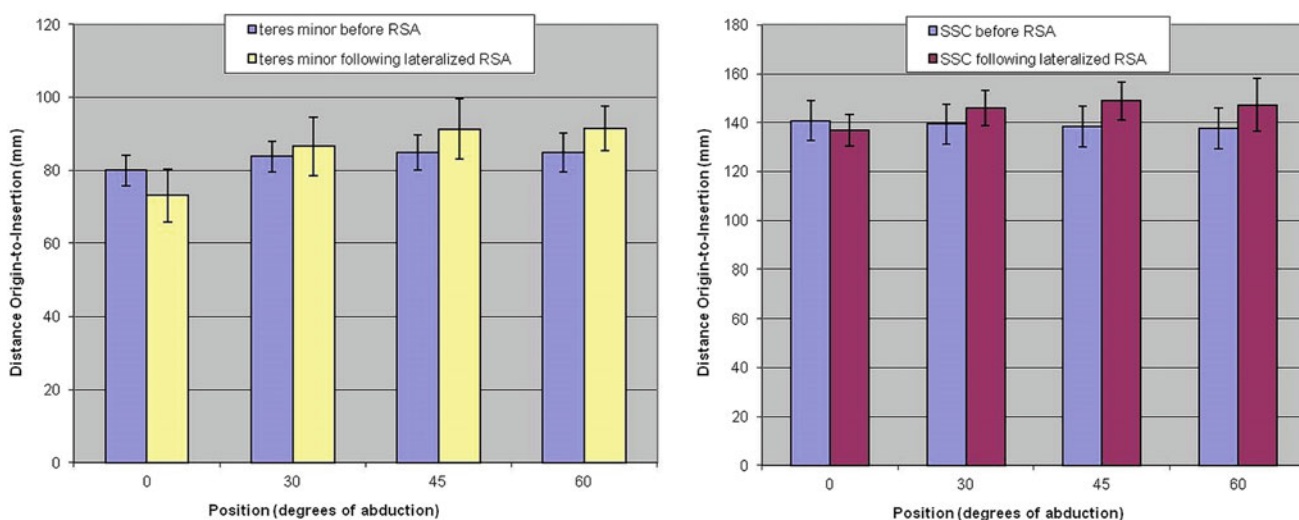


Fig. 2.5 Muscle length measured as distance from origin to insertion (mm) of teres minor and subscapularis before and after lateralized RSA. At the 0° position, muscle length shows slightly smaller values, whereas for all other positions, an increase of muscle length can be seen

reduced by an average of 30 % compared to the normal shoulder with an intact rotator cuff. However, this reduction applies to compression forces to the glenoid in particular, whereas superiorly directed shear forces might increase. With forward flexion, an increase of posterior shear forces to the glenoid of up to 41 % bodyweight is observed [38].

Kinematic Analysis of RSA

The key features of conventional, “Grammont type,” RSA design are additional to the reversed hemispheric design, the medialization of the COR, the use of a larger ball on the glenoid component, the implementation of 155° nonanatomic humeral inclination and the distalization of the deltoid. These changes lead to significant improvement of shoulder function, especially in patients with cuff tear arthropathy [48–50]. On the other hand, implant-related problems such as inferior scapular notching or postoperatively reduced external or internal rotation arise. Kinematic analysis of RSA has identified the reason for these problems, and possible solutions are consequence of this work.

One of the main aspects is related to prosthetic design in RSA in the impingement-free range of motion and occurrence of inferior scapular notching as a possible result of inferior impingement [51, 52]. While other factors such as polyethylene wear or rotational impingement might contribute to the development or progression of scapular notching, the contact of the humeral polyethylene liner with the inferior scapular neck is believed to be the most important factor [51]. In conventional reverse shoulder arthroplasty, the COR is shifted medially to avoid shear forces between the glenoid component and the glenoid. The lack in lateral offset and the semiconstrained design leads to a contact of the medial border of the humeral component with the inferior scapular neck in adduction position of the arm. The minimal abduction angle at which this contact occurs depends on factors such as implant design and positioning. Different strategies have been proposed to avoid this: One is to place the glenoid component in a more inferior position with or without an inferior tilt [40, 53], and the other is to lateralize the COR. Conventional “Grammont-type” reverse shoulder arthroplasty, where a 36-mm glenoid component is implanted centrally on the glenoid, has a minimal abduction angle of about 30° and a maximum impingement-free abduction of 85°–95° [54, 55]. Placing the glenoid component more inferiorly, so an inferior overhang of the glenosphere occurs, leads to significantly decreased minimal adduction angles. There seems to be a direct correlation between the amount of distalization and the minimal abduction angle. Shifting the glenoid component from a central position to a position, where the glenosphere is flush with the scapular neck, results in a

decrease of minimal abduction angle from 25° to 11°. Implanting the glenoid component even further distally, so a slight overhang is apparent and further decreases the angle to 1° [53]. Other authors confirm these finding, but suggest that dependant on the amount of distalization, there still might be an inferior scapular impingement at an abduction angle of about 1°–9° [53, 55].

Shifting the COR laterally has proven to be effective in decreasing the minimal abduction angle and the overall range of motion. A 10 mm lateralization does decrease minimal abduction angle by about 15°. Nonetheless, inferior mechanical conflict will still occur at about 12° of abduction [55]. Berhouet found a decrease of adduction deficit of 10° with a 7-mm lateral offset 36-mm glenoid component [56].

Tilting the glenoid component inferiorly does also lead to a decrease of minimal abduction angle. Gutiérrez et al. report on a 16° decrease with a 15° inferior tilt, compared with the glenosphere being in a superiorly facing position [55]. Comparing a glenoid component implanted in neutral position with an 10°–15° inferior tilted glenosphere, the decrease of minimal abduction angle is smaller: Nyffeler et al. found a 5° decrease comparing a neutral glenoid component position with the glenosphere implanted with inferior tilt [53]. The same amount was seen by Berhouet et al. [56].

Choosing a bigger glenosphere does also lead to decreased adduction deficit. With a 42-mm glenoid component adduction deficit decreases by 5° compared to a 30-mm glenosphere. Berhouet even found a decrease of 10°, when going from a 36- to 42-mm component. While these data suggest that the size of the glenoid component has only a small effect compared to other surgical strategies such as tilting or inferior offsetting, the effect might be much bigger in clinical practice: The bigger glenosphere allows a substantially bigger inferior overhang with the same baseplate position; thus, the effect of glenoid component size and distal overhang might add up to a more decreased minimal abduction angle.

With all of the above-mentioned strategies, a small adduction deficit of various degrees will most likely remain. Applying these strategies in combination can fully eliminate inferior impingement in the majority of patients. Implanting a glenoid component with 10-mm lateral offset with an inferior overhang will fully eliminate adduction deficit [55] (Fig. 2.6). The same result can be achieved using a 42-mm glenosphere with a 10-mm offset or with combination of a centrally implanted 36-mm glenosphere with a 10-mm offset and inferior tilt [56]. In a comparative study, Roche et al. compares the combined effect of these strategies: The biggest gain in overall range of motion can be achieved by combination of inferior shift and lateral offset. Placing a 36-mm glenosphere from a central position to a 6-mm inferior offset position and increasing lateral offset by 6 mm resulted in an overall gain in range of motion from 59° to 109° [57].

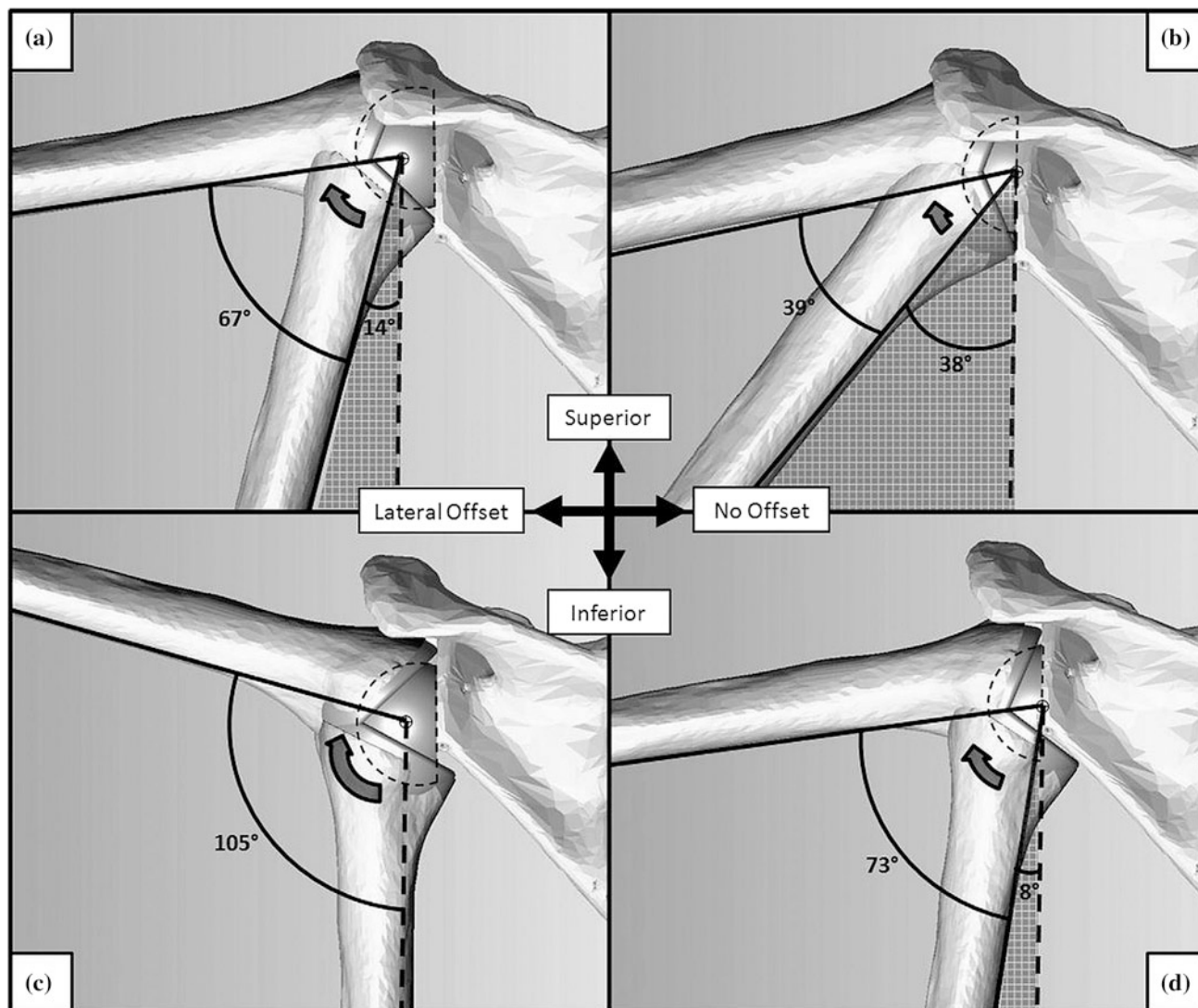


Fig. 2.6 Effect of glenosphere position relative to the glenoid and lateral offset of the glenosphere on impingement-free range of motion [55]

Rotation of the humeral component has no significant effect on the overall range of motion. Nonetheless, when the humeral component is implanted in 40° retroversion, inferior impingement occurred earlier compared to 10° or 20° retroversion. Usage of a 42-mm glenoid component fully eliminates this finding. On the other hand, inferior impingement occurs the earliest with the highly retroverted positions compared to the 10° or anatomic versions, unless a centered 36 mm tilted or neutrally implanted glenosphere is used, where again no effect of the humeral components version can be seen [56].

References

1. Carbone S, Postacchini R, Gumina S. Scapular dyskinesis and SICK syndrome in patients with a chronic type III acromioclavicular dislocation. Results of rehabilitation. *Knee Surg Sports Traumatol Arthrosc.* 24 Jan 2014.
2. Su WR, Budoff JE, Luo ZP. The effect of coracoacromial ligament excision and acromioplasty on superior and anterosuperior glenohumeral stability. *Arthroscopy.* 2009;25(1):13–8.
3. Wu CH, Chang KV, Su PH, Kuo WH, Chen WS, Wang TG. Dynamic ultrasonography to evaluate coracoacromial ligament displacement during motion in shoulders with supraspinatus tendon tears. *J Orthop Res.* 2012;30(9):1430–4.

4. Checroun AJ, Hawkins C, Kummer FJ, Zuckerman JD. Fit of current glenoid component designs: an anatomic cadaver study. *J Shoulder Elbow Surg.* 2002 Nov–Dec;11(6):614–7. American Shoulder and Elbow Surgeons.
5. Churchill RS, Brems JJ, Kotschi H. Glenoid size, inclination, and version: an anatomic study. *J Shoulder Elbow Surg.* 2001 Jul–Aug;10(4):327–32. American Shoulder and Elbow Surgeons.
6. Torrens C, Corrales M, Gonzalez G, Solano A, Caceres E. Cadaveric and three-dimensional computed tomography study of the morphology of the scapula with reference to reversed shoulder prosthesis. *J Orthop Surg Res.* 2008;3:49.
7. Paisley KC, Kraeutler MJ, Lazarus MD, Ramsey ML, Williams GR, Smith MJ. Relationship of scapular neck length to scapular notching after reverse total shoulder arthroplasty by use of plain radiographs. *J Shoulder Elbow Surg.* 2014 Jun;23(6):882–7. American Shoulder and Elbow Surgeons.
8. Habermeyer P, Magosch P, Luz V, Lichtenberg S. Three-dimensional glenoid deformity in patients with osteoarthritis: a radiographic analysis. *J Bone Joint Surg Am.* 2006;88(6):1301–7.
9. Lewis GS, Armstrong AD. Glenoid spherical orientation and version. *J Shoulder Elbow Surg.* 2011 Jan;20(1):3–11. American Shoulder and Elbow Surgeons.
10. Friedman RJ, Hawthorne KB, Genev BM. The use of computerized tomography in the measurement of glenoid version. *J Bone Joint Surg Am.* 1992;74(7):1032–7.
11. Frankle MA, Teramoto A, Luo ZP, Levy JC, Pupello D. Glenoid morphology in reverse shoulder arthroplasty: classification and surgical implications. *J Shoulder Elbow Surg.* 2009;18(6):874–85. American Shoulder and Elbow Surgeons.
12. Monk AP, Berry E, Limb D, Soames RW. Laser morphometric analysis of the glenoid fossa of the scapula. *Clin Anat (New York, NY).* 2001 Sep;14(5):320–3.
13. Hoenecke HR, Jr, Hermida JC, Flores-Hernandez C, D'Lima DD. Accuracy of CT-based measurements of glenoid version for total shoulder arthroplasty. *J Shoulder Elbow Surg.* 2010 Mar;19(2):166–71. American Shoulder and Elbow Surgeons.
14. Herrmann S, König C, Perka C, Greiner S, editors. Korrelation zwischen Muskeldegeneration der Rotatorenmanschette und Glenoidmorphologie bei degenerativen Schultergelenkerkrankungen Meeting Presentation, Deutscher Kongress für Orthopädie und Unfallchirurgie (DKOU 2012); 2012; Berlin.
15. Walch G, Badet R, Boulahia A, Khoury A. Morphologic study of the glenoid in primary glenohumeral osteoarthritis. *J Arthroplasty.* 1999;14(6):756–60.
16. Boileau P, Walch G. The three-dimensional geometry of the proximal humerus. Implications for surgical technique and prosthetic design. *J Bone Joint Surg Br.* 1997;79(5):857–65.
17. Hernigou P, Duparc F, Hernigou A. Determining humeral retroversion with computed tomography. *J Bone Joint Surg Am.* 2002 Oct;84-A(10):1753–62.
18. Soslowsky LJ, Flatow EL, Bigliani LU, Mow VC. Articular geometry of the glenohumeral joint. *Clin Orthop Relat Res.* 1992;285:181–90.
19. Kwon YW, Powell KA, Yum JK, Brems JJ, Iannotti JP. Use of three-dimensional computed tomography for the analysis of the glenoid anatomy. *J Shoulder Elbow Surg.* 2005 Jan–Feb;14(1):85–90. American Shoulder and Elbow Surgeons.
20. Snyder SJ, Karzel RP, Del Pizzo W, Ferkel RD, Friedman MJ. SLAP lesions of the shoulder. *Arthroscopy.* 1990;6(4):274–9.
21. Maffet MW, Gartsman GM, Moseley B. Superior labrum-biceps tendon complex lesions of the shoulder. *Am J Sports Med.* 1995 Jan–Feb;23(1):93–8.
22. O'Brien SJ, Neves MC, Arnoczky SP, Rozbruch SR, Dicarlo EF, Warren RF, et al. The anatomy and histology of the inferior glenohumeral ligament complex of the shoulder. *Am J Sports Med.* 1990 Sep–Oct;18(5):449–56.
23. Mochizuki T, Sugaya H, Uomizu M, Maeda K, Matsuki K, Sekiya I, et al. Humeral insertion of the supraspinatus and infraspinatus. New anatomical findings regarding the footprint of the rotator cuff. *J Bone Joint Surg Am.* 2008;90(5):962–9.
24. Richards DP, Burkhart SS, Tehrany AM, Wirth MA. The subscapularis footprint: an anatomic description of its insertion site. *Arthroscopy.* 2007;23(3):251–4.
25. Arai R, Sugaya H, Mochizuki T, Nimura A, Moriishi J, Akita K. Subscapularis tendon tear: an anatomic and clinical investigation. *Arthroscopy.* 2008;24(9):997–1004.
26. Leijnse JN, Han SH, Kwon YH. Morphology of deltoid origin and end tendons—a generic model. *J Anat.* 2008;213(6):733–42.
27. Lorne E, Gagey O, Quillard J, Hue E, Gagey N. The fibrous frame of the deltoid muscle. Its functional and surgical relevance. *Clin Orthop Relat Res.* 2001;386:222–5.
28. Rispoli DM, Athwal GS, Sperling JW, Cofield RH. The anatomy of the deltoid insertion. *J Shoulder Elbow Surg.* 2009 May–Jun;18(3):386–90. American Shoulder and Elbow Surgeons.
29. Radkowski CA, Richards RS, Pietrobon R, Moorman CT III. An anatomic study of the cephalic vein in the deltopectoral shoulder approach. *Clin Orthop Relat Res.* 2006;442:139–42.
30. Sahara W, Sugamoto K, Murai M, Tanaka H, Yoshikawa H. The three-dimensional motions of glenohumeral joint under semi-loaded condition during arm abduction using vertically open MRI. *Clin Biomech (Bristol, Avon).* 2007 Mar;22(3):304–12.
31. Lippitt SB, Vanderhooft JE, Harris SL, Sidles JA, Harryman DT, II, Matsen FA, III. Glenohumeral stability from concavity-compression: a quantitative analysis. *J Shoulder Elbow Surg.* 1993 Jan;2(1):27–35. American Shoulder and Elbow Surgeons.
32. Apreleva M, Parsons IM, Warner JJ, Fu FH, Woo SL. Experimental investigation of reaction forces at the glenohumeral joint during active abduction. *J Shoulder Elbow Surg.* 2000 Sep–Oct;9(5):409–17. American Shoulder and Elbow Surgeons.
33. Parsons IM, Apreleva M, Fu FH, Woo SL. The effect of rotator cuff tears on reaction forces at the glenohumeral joint. *J Orthop Res.* 2002;20(3):439–46.
34. Ruckstuhl H, Krzycki J, Petrou N, Favre P, Horn T, Schmid S, et al. Shoulder abduction moment arms in three clinically important positions. *J Shoulder Elbow Surg.* 2009 Jul–Aug;18(4):632–8. American Shoulder and Elbow Surgeons.
35. Ackland DC, Richardson M, Pandy MG. Axial rotation moment arms of the shoulder musculature after reverse total shoulder arthroplasty. *J Bone Joint Surg Am.* 2012;94(20):1886–95.
36. Herrmann S, König C, Heller M, Perka C, Greiner S. Reverse shoulder arthroplasty leads to significant biomechanical changes in the remaining rotator cuff. *J Orthop Surg Res.* 2011;6(1):42.
37. Otis JC, Jiang CC, Wickiewicz TL, Peterson MG, Warren RF, Santner TJ. Changes in the moment arms of the rotator cuff and deltoid muscles with abduction and rotation. *J Bone Joint Surg Am.* 1994;76(5):667–76.
38. Kontaxis A, Johnson GR. The biomechanics of reverse anatomy shoulder replacement—a modelling study. *Clin Biomech (Bristol, Avon).* 2009 Mar;24(3):254–60.
39. De Wilde LF, Audenaert EA, Berghs BM. Shoulder prostheses treating cuff tear arthropathy: a comparative biomechanical study. *J Orthop Res.* 2004;22(6):1222–30.
40. Boileau P, Watkinson DJ, Hatzidakis AM, Balg F. Grammont reverse prosthesis: design, rationale, and biomechanics. *J Shoulder Elbow Surg.* 2005;14(1 Suppl S):147S–61S. American Shoulder and Elbow Surgeons.
41. Simovitch RW, Helmy N, Zumstein MA, Gerber C. Impact of fatty infiltration of the teres minor muscle on the outcome of reverse total shoulder arthroplasty. *J Bone Joint Surg Am.* 2007;89(5):934–9.

42. Edwards TB, Williams MD, Labriola JE, Elkousy HA, Gartsman GM, O'Connor DP. Subscapularis insufficiency and the risk of shoulder dislocation after reverse shoulder arthroplasty. *J Shoulder Elbow Surg.* 2009 Nov-Dec;18(6):892–6. American Shoulder and Elbow Surgeons.
43. Werner CM, Steinmann PA, Gilbert M, Gerber C. Treatment of painful pseudoparesis due to irreparable rotator cuff dysfunction with the Delta III reverse-ball-and-socket total shoulder prosthesis. *J Bone Joint Surg Am.* 2005;87(7):1476–86.
44. Clark JC, Ritchie J, Song FS, Kissenberth MJ, Tolan SJ, Hart ND, et al. Complication rates, dislocation, pain, and postoperative range of motion after reverse shoulder arthroplasty in patients with and without repair of the subscapularis. *J Shoulder Elbow Surg.* 2011. American Shoulder and Elbow Surgeons.
45. Boileau P, Moineau G, Roussanne Y, O'Shea K. Bony increased-offset reversed shoulder arthroplasty: minimizing scapular impingement while maximizing glenoid fixation. *Clin Orthop Relat Res.* 2011;469(9):2558–67.
46. Greiner S, Schmidt C, König C, Perka C, Herrmann S. Lateralized reverse shoulder arthroplasty maintains rotational function of the remaining rotator cuff. *Clin Orthop Relat Res.* 2013;471(3):940–6.
47. Bergmann G, Graichen F, Bender A, Rohlmann A, Halder A, Beier A, et al. In vivo gleno-humeral joint loads during forward flexion and abduction. *J Biomech.* 2011;44(8):1543–52.
48. Boileau P, Watkinson D, Hatzidakis AM, Hovorka I. Neer Award 2005: The Grammont reverse shoulder prosthesis: results in cuff tear arthritis, fracture sequelae, and revision arthroplasty. *J Shoulder Elbow Surg.* 2006 Sept-Oct;15(5):527–40. American Shoulder and Elbow Surgeons.
49. Cuff D, Pupello D, Virani N, Levy J, Frankle M. Reverse shoulder arthroplasty for the treatment of rotator cuff deficiency. *J Bone Joint Surg Am.* 2008;90(6):1244–51.
50. Grassi FA, Murena L, Valli F, Alberio R. Six-year experience with the Delta III reverse shoulder prosthesis. *J Orthop Surg (Hong Kong).* 2009;17(2):151–6.
51. Levigne C, Boileau P, Favard L, Garaud P, Mole D, Sirveaux F, et al. Scapular notching in reverse shoulder arthroplasty. *J Shoulder Elbow Surg.* 2008 Nov-Dec;17(6):925–35. American Shoulder and Elbow Surgeons.
52. Simovitch RW, Zumstein MA, Lohri E, Helmy N, Gerber C. Predictors of scapular notching in patients managed with the Delta III reverse total shoulder replacement. *J Bone Joint Surg Am.* 2007;89(3):588–600.
53. Nyffeler RW, Werner CM, Gerber C. Biomechanical relevance of glenoid component positioning in the reverse Delta III total shoulder prosthesis. *J Shoulder Elbow Surg.* 2005 Sep-Oct;14(5):524–8. American Shoulder and Elbow Surgeons.
54. Roche CP, Marczuk Y, Wright TW, Flurin PH, Grey SG, Jones RB, et al. Scapular notching in reverse shoulder arthroplasty: validation of a computer impingement model. *Bull Hosp Joint Dis.* 2013;71(4):278–83.
55. Gutierrez S, Comiskey CA, Luo ZP, Pupello DR, Frankle MA. Range of impingement-free abduction and adduction deficit after reverse shoulder arthroplasty. Hierarchy of surgical and implant-design-related factors. *J Bone Joint Surg Am.* 2008;90(12):2606–15.
56. Berhouet J, Garaud P, Favard L. Evaluation of the role of glenosphere design and humeral component retroversion in avoiding scapular notching during reverse shoulder arthroplasty. *J Shoulder Elbow Surg.* 2014 Feb;23(2):151–8. American Shoulder and Elbow Surgeons.
57. Roche C, Flurin PH, Wright T, Crosby LA, Mauldin M, Zuckerman JD. An evaluation of the relationships between reverse shoulder design parameters and range of motion, impingement, and stability. *J Shoulder Elbow Surg.* 2009 Sep-Oct;18(5):734–41. American Shoulder and Elbow Surgeons.

Reverse Shoulder Arthroplasty
Biomechanics, Clinical Techniques, and Current
Technologies

Frankle, M.; Marberry, S.; Pupello, D. (Eds.)

2016, XVII, 486 p., Hardcover

ISBN: 978-3-319-20839-8